



Filter Design for Optically Recorded Cardiac Electrical Activity Recorded During Ischemia

Fei Xie^a, Christian Zemlin^{b*}

^aDepartment of Electrical and Computer Engineering, Old Dominion University, Norfolk, VA

^bFrank Reidy Center for Bioelectrics, Old Dominion University, Norfolk, VA

^aEmail: robinxie21@gmail.com

^bEmail: czemlin@odu.edu

Abstract

Optical mapping provides two-dimensional recordings of cardiac electric activity that vary in time. If it is employed to study ischemia, filters should be designed to preserve the maximum slope of the action potential as much as possible. We evaluate temporal filters (low-pass and temporal averaging with different radii) and find that the. Spatial filters (spatial averaging with different radii and constant or Gaussian weights) generally gave good results both for maximum slope preservation and signal-to-noise ratio (SNR) increase. Spatial averaging with radius 2, in particular achieved a SNR of 65 for synthetic data and 40 for real data while reducing the maximum slope by less than 20%; it also results in high-quality action potential waveform, activation map, and action potential duration map. We conclude that spatial averaging with radius 2 is an appropriate filter for optical mapping with our system.

Keywords: Type your keywords here, separated by semicolons.

1. Introduction

Cardiac ischemia is a restriction of blood supply to the heart, which occurs when a coronary vessel is partially or completely blocked, e.g. by atherosclerosis or a thrombus.

* Corresponding author.

E-mail address: czemlin@odu.edu .

While restoration of blood supply is usually the goal of ischemia treatment, the reperfusion of ischemic tissue can cause additional damage known as reperfusion injury [1].

Because of the high prevalence and severity of ischemia, animal models have been developed to study the mechanisms of ischemia and develop reperfusion approaches that avoid or minimize reperfusion injury [2-4].

A convenient technique to study ischemia in isolated animal hearts is optical mapping, which uses voltage-sensitive fluorescent probes to convert electrical activity into optical signals that can be recorded with fast, sensitive cameras [5-7]. Optical mapping signals are, however, noisy and should be filtered to obtain acceptable signal-to-noise ratios (SNRs). At the same time, filters should be chosen in a way that minimizes alterations to the underlying signal; in the case of ischemia it is especially important to preserve the maximum slope of the action potential upstroke of the underlying signal, because it is a measure of the degree of ischemia.

Here, we study the effect of low-pass filtering, temporal averaging, and spatial averaging on optical mapping movies, both in synthetic data and in data recorded from optical mapping experiments. Synthetic data consist of simulated cardiac activity with added noise; for these data, it is easily possible to quantify the distortion because the undistorted signal is available. Our goal is to determine a filtering scheme that reaches a high SNR; we consider 30-35 an acceptable value. At the same time, we want to minimize the reduction in maximum slope and do not accept a reduction by more than 25%.

2. Materials and Methods

2.1. Experimental recording of action potentials

All experiment protocols conformed to National Institutes of Health guidelines and followed our approved animal protocol. The hearts of adult New Zealand rabbits (n=3) were surgically removed, the aorta immediately cannulated, and the heart flushed with and immersed in cold cardioplegic solution (in mM: glucose 280, KCl 13.4, NaHCO₃ 12.6, mannitol 34). Hearts were placed in an optical mapping setup and retrogradely perfused with Tyrode solution (in mM: NaCl 130, KCl 4.0, CaCl₂ 1.8, MgCl₂ 1.0, NaHCO₃ 24, NaH₂PO₄ 1.2, glucose 5.6) and bubbled with 95% O₂/5% CO₂ at a pressure of 60-80 mmHg, with pH kept between 7.35 and 7.45 and temperature 37.5±0.5°C.

Optical mapping was performed after injecting a 5 ml bolus of the voltage-sensitive fluorescent probe di-4-ANEPPS (10µM). The electro-mechanical uncoupler blebbistatin (10µmol/L) was added to the Tyrode solution to reduce motion artifacts. As shown in Fig. 1, the heart was illuminated with a 532 nm, 1000 mW, diode-pumped solid-stated laser (Shanghai Dream Lasers), which was diffused and directed towards the heart via a dichroic mirror. Fluorescence was recorded through a 715 nm LP filter at 1000 frames/s with a CCD camera (Little Joe, SciMeasure).

2.2 Synthetic data and filtering

Synthetic data were generated by simulating electrical activity in a sheet of cardiac tissue with the Luo-Rudy

model [8]. Simulations were performed on a 300 x 300 pixel medium with a time step of 10 μs and a space step of 100 μm. The medium was stimulated in the center, and the synthetic data were taken from the point of stimulation with a sampling frequency of 1000 Hz. White noise was added using Matlab's random number generator. Temporal and spatial averaging filters of all radii used uniform weights that were normalized (i.e. their sum was 1) in all cases. The Gaussian filter we used had standard deviation σ=1.475 and was represented by the following 7x7 matrix:

$$G_7 = \frac{1}{264} \begin{pmatrix} 0 & 1 & 2 & 3 & 2 & 1 & 0 \\ 1 & 3 & 6 & 8 & 6 & 3 & 1 \\ 2 & 6 & 13 & 16 & 13 & 6 & 2 \\ 3 & 8 & 16 & 20 & 16 & 8 & 3 \\ 2 & 6 & 13 & 16 & 13 & 6 & 2 \\ 1 & 3 & 6 & 8 & 6 & 3 & 1 \\ 0 & 1 & 2 & 3 & 2 & 1 & 0 \end{pmatrix}.$$

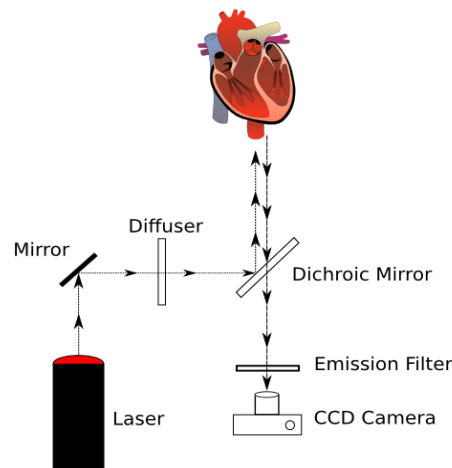


Figure 1. Schematic diagram of the optical setup. Arrows indicate the direction of light propagation.

2.3 Determination of SNR and maximum slope

The signal amplitude was determined by subtracting the minimum of the signal (over one action potential) from the maximum of the signal, the noise level was defined as the amplitude of the signal during the resting phase (after the action potential, when the noise-free signal would be constant). To determine the SNR, we divide the signal amplitude by the noise level.

The maximum slope is computed by finding the maximum of $(V(t)-V(\Delta t))/\Delta t$ of the signal. We chose $\Delta t=7$ ms in all our computations.

2.4 Noise analysis

The camera is a main source of noise in the optical mapping, and the noise it produces can be conveniently characterized. We computed the temporal and spatial autocorrelation functions of the camera noise.

$$A_t(\Delta t) = \frac{1}{N} \sum_{t=0}^{N-1} x_1[t]x_1[t+k]$$

$$A_s(\Delta x) = \frac{1}{N} \sum_{n=0}^{N-1} x_1[n]x_1[n+k]$$

where $A_t(\Delta t)$ and $A_s(\Delta x)$ is the autocorrelation of the camera noise in time and in space, respectively. N is the number of samples, x_1 is the camera noise, and k is the shift of the signal. To normalize the autocorrelation, we divided by the variance.

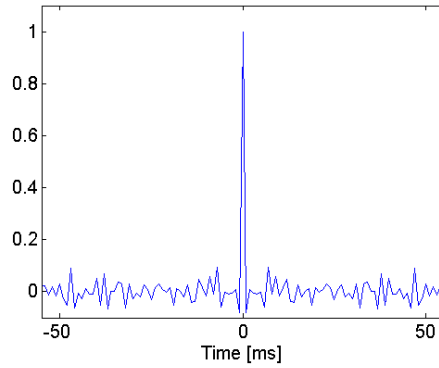


Figure 2. Autocorrelation of the camera noise in time.

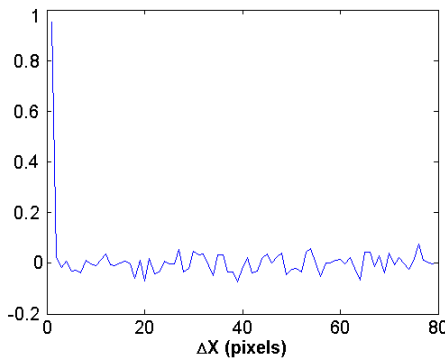


Figure 3. Autocorrelation of the camera noise in space.

3. Results

3.1 Autocorrelation of camera noise

Figures 2 and 3 show the autocorrelation of the camera signal in the absence of a stained heart, both in time and in space. The autocorrelation drops to zero immediately both in time and space: The same pixel in subsequent

frames is uncorrelated, and so are adjacent pixels in the same frame. This justifies the use of white noise in the generation of our synthetic signals.

3.2 Low-pass filters

Figure 4 shows the power spectrum density of the signal (stimulated heart is present) and noise (stimulated heart is absent).

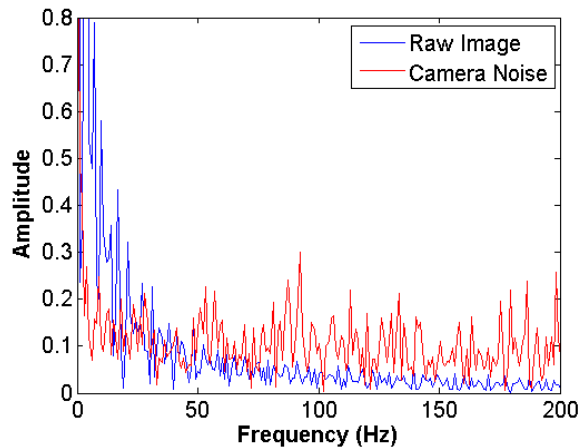


Figure 4. Power spectrum density of raw image and camera noise.

It is apparent that the signal does not contain significant components above ~40 Hz so that low-pass filtering is a promising strategy. Figure 5 shows how maximum slope and SNR are affected by low-pass filters of different cutoff frequencies (generated by Matlab).

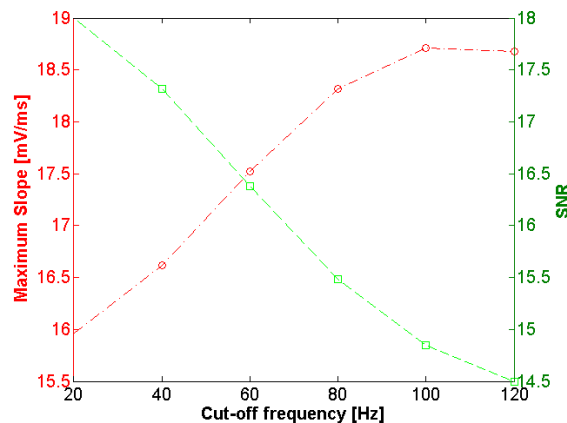


Figure 5. Slope and SNR vs cut-off frequency for low-passed filtered synthetic data

The maximum slope is only mildly affected by the low-pass filtering: For a cutoff at 120 Hz the maximum slope is 18.6 mV/ms, for 20 Hz, the most aggressive cutoff tested, it is still 16 mV/ms. The improvement in SNR is likewise modest: For a cutoff at 120 Hz, we have SNR=14.5, while a cutoff of 20 Hz yields SNR=18.

In conclusion, low-pass filters designed to leave the main components of the signal intact do not sufficiently improve the SNR.

3.3. Temporal averaging filters

Figure 6 shows how temporal averaging affects maximum slope and SNR for different filter radii. A filter of radius $r=7$ increases the SNR to 26, which is not sufficient for us, while the maximum slope has already dropped to ~ 8 mV/ms, which is less than half of the unfiltered maximum slope (22.2 mV/ms), an unacceptable reduction.

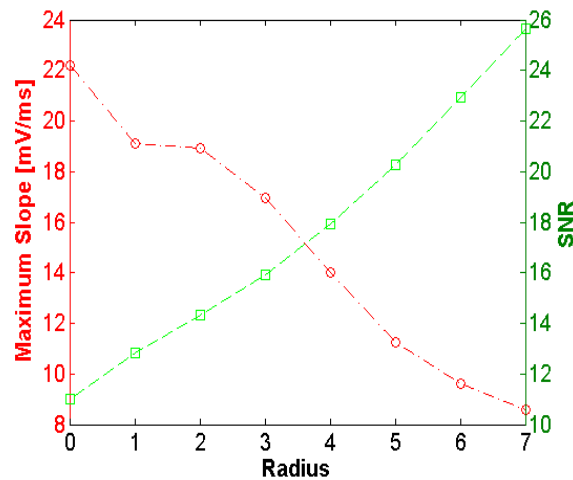


Figure 6. Slope and SNR vs. filter radius for time-averaged synthetic data.

It is intuitive that temporal averaging would strongly affect the maximum slope of a signal, because it is designed to even out differences in time; at the same time, the SNR gain is modest because the averaging occurs in one dimension (time), so that the number of pixels over which averaging occurs grows linearly with the filter radius, as opposed to spatial filtering where the number grows quadratically (in two-dimensional media).

3.4. Spatial averaging filters

Figure 7 shows our results for spatial filtering. The maximum slope of the unfiltered signal was 20.5 mV/ms, it was reduced to approximately 18 mV/ms for a $r=2$ and to 13 mV/ms for a $r=7$.

At the same time, the SNR increased approximately linearly with the filter radius from its original value of 12, measuring 65 at $r=2$ and 330 at $r=7$. This excellent performance has two reasons: First, the number of pixels over which averaging is performing grows quadratically with radius so that a rapid increase of SNR with radius can be expected. At the same time, the maximum slope should be much less affected by spatial than by temporal filtering. If, for example, all pixels were excited in synchrony, spatial filtering would not reduce the maximum slope at all. The mild reduction that we observe is most likely a consequence of the fact that our test signal was a propagating wave, so that there is a small shift in the activation times of neighboring pixels.

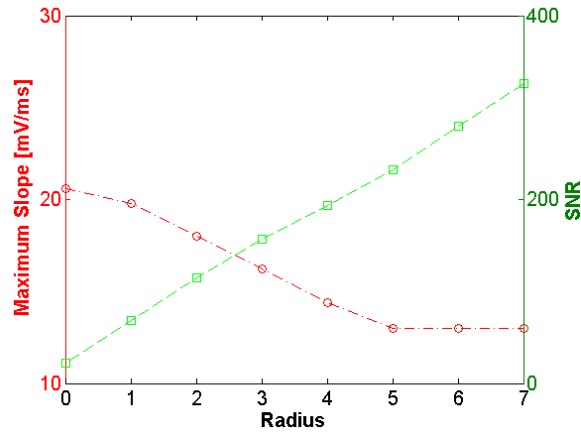


Figure 7. Slope and SNR vs. filter radius for spatially averaged synthetic data.

Beyond spatial averaging filters, we also tested 7x7 ($r=3$) Gaussian convolution kernel spatial filters (standard deviation $\sigma=1.475$), with likewise good results. Table 1 shows a comparison of the $r=2$ Gaussian filter with $r=2$ and $r=3$ spatial averaging filters. We see that the $r=2$ Gaussian filter and the $r=2$ averaging filter give very similar results, while the $r=3$ averaging filter substantially reduces the slope for just a small increase in SNR. We favor the $r=2$ averaging filter because of its simplicity.

Table 1: Comparison of spatial filters

	SNR	Slope
Radius=2 constant	41.96	145
Radius=3 Gaussian	41.82	160
Radius=3 constant	45.99	117.2

3.5. Testing on real data: Maximum slope and SNR

Figure 8 shows the effect of spatial averaging ($r=2$) on maximum slope and SNR for real optical mapping data.

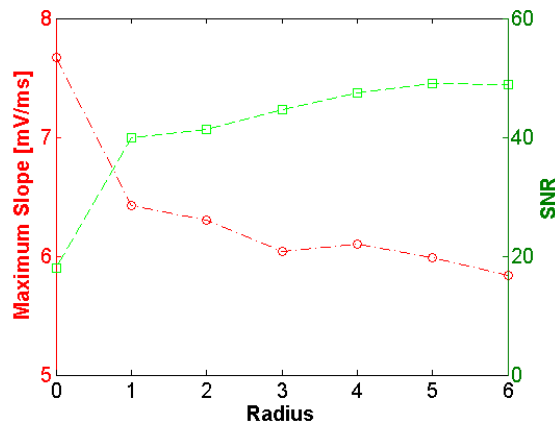


Figure 8. Slope and SNR vs. filter radius for spatially averaged real data.

As for the synthetic data, the maximum slope is not affected very much, it decreases from its initial value of 7.7 mV/ms to 6.3 mV/ms at $r=2$ and 5.9 mV/ms for $r=6$. The slopes in real data are generally much lower than in synthetic data; this is a known limitation of optical mapping that stems from photon diffusion⁹. The SNR grows rapidly, from ~ 18 for the raw data to ~ 40 for $r=2$ and ~ 50 for $r=6$. The SNR does not grow as consistently as for the synthetic data show in Fig. 7; this suggests that the optical mapping signal contains other noise besides the white noise added to the synthetic signal. At any rate, the results for SNR with spatial filters of radius greater or equal to 2 are acceptable to us.

3.6. Testing on real data: action potentials, activation maps, and amplitude maps

Figure 9 shows the effect of two ways of spatial averaging on real action potentials. The original signal is shown in Panel a. Panel b shows the same signal spatially averaged with $r=2$; Panel c with Gaussian filtering ($r=3$). Both filters exhibit a substantially reduced noise level with no discernible change in signal slope. There is no apparent difference in the quality of the two filters.

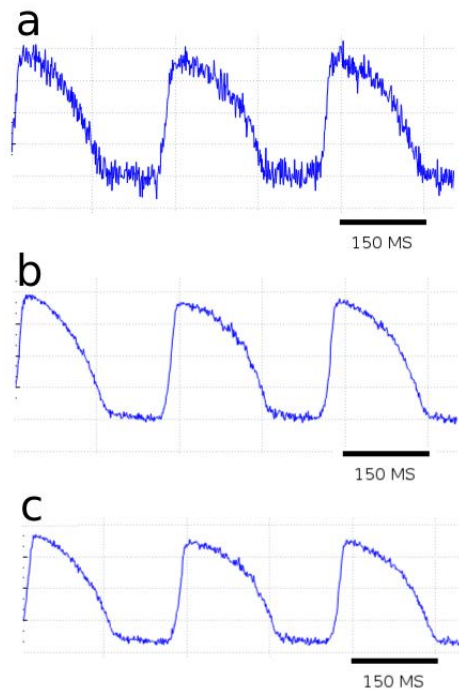


Figure 9. (a) Representative raw optical action potential from a single pixel location; (b) the signal following $r=2$ spatial filtering; (c) the signal following $r=3$ Gaussian convolution spatial filtering.

Another important mode of evaluation of cardiac activity are activation maps. An activation map illustrates the order in which different points of the cardiac surface are electrically activated (i.e. the local voltage increases from resting level to excited level). Figure 10 shows activation maps computed for on original movie of cardiac activation (Panel a) and activation maps for the same data after spatial averaging with radius 2. In both panels it can be seen that the earliest activation (darkest shade of gray) occurs slightly above the center of the field of view. The unfiltered image is, however, noisy and speckled, and especially at the periphery of the heart, there are missing pixels because high noise levels and low illumination make a determination of activation time

imprecise. In the filtered image, the activation map extends smoothly to the edge of the heart and gives a clear illustration of the activation sequence.

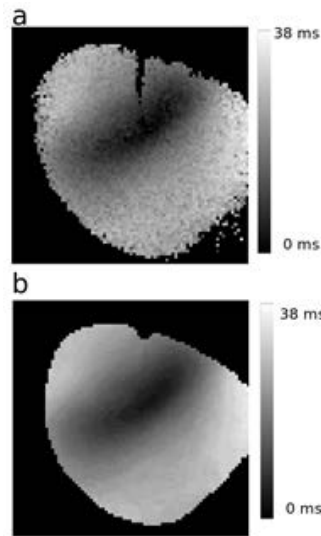


Figure 10. Activation Map: (a) from unfiltered signal; (b) from spatially averaged signal ($r=2$).

Figure 11 shows the action potential duration (APD) map for unfiltered and filtered signals. Similar to the activation map, the APD map of the unfiltered signal (Panel A) is speckled and it is not possible to detect small regional variations in APD. The filtered APD map (APD) is smooth and shows clearly that the APD is reduced in the vicinity of the stimulation site. The filtered image can also be “stretched”, i.e. its grayscale values can be linearly rescaled to cover the whole available range from black to white (this is not useful for the unfiltered image because due to the noise, the available grayscale range is already being used). The stretched image (Panel c) achieves substantially better resolution and uncovers regional variation in the APD.

4. Discussion

In this paper, we tested a variety of filters to improve the SNR of optical mapping signals. Since we are planning to use optical mapping for the study of ischemia, and this requires careful measurement of the maximum slope of the action potential, we were interested in filters that minimize the change in action potential slope.

Our results show that temporal filters, low-pass filtering as well as temporal averaging, perform poorly for our purposes. In low-pass filtering, we cannot obtain a SNR above 18 without filtering out major signal components, for temporal filtering, only aggressive radii of 5 or more push the SNR above 20, while the maximum slope is reduce to a fraction of its original value.

Spatial filters, on the other hand, can meet all our requirements. Spatial averaging with radius 2 in particular achieves an increase from ~ 12 to ~ 50 for synthetic data and ~ 18 to ~ 40 for real optical mapping data. At the same time, the maximum slope is largely preserved; it drops by less than 20% in either case. Gaussian spatial filters achieved results that were equivalent to spatial averaging.

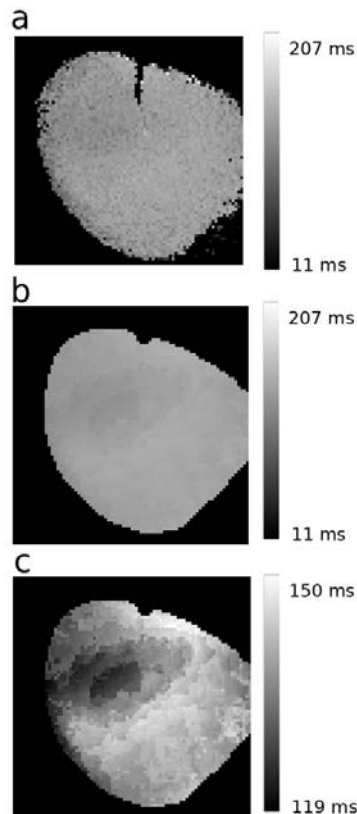


Figure 11. APD map: (a) from unfiltered signal; (b) from spatially averaged signal ($r=2$); (c) from spatially averaged signal with rescaled color bar.

In more detailed tests of spatial averaging with radius 2, we found that in the action potential wave form, activation map, and APD map all have excellent quality for the real optical mapping data we used as input.

The main limitation of this paper is that we restricted ourselves to relatively simple kinds of filters (low-pass, averaging, and Gaussian filters); more sophisticated filters based on spatial Fourier transforms may be able to get even better results. Also, our synthetic data generation did not incorporate the photon dynamics inside the tissue; more advanced synthetic data generation that does include them would be able to get a closer match between synthetic and real data.

5. Conclusions

For optical mapping experiments of ischemia, which require both high SNR and preservation of the action potential maximum slope, spatial filters perform well while temporal filters are inadequate. Spatial averaging with radius 2, in particular resulted in high-quality signals, activation maps, and APD maps.

References

- [1] K. R. Bainey and P. W. Armstrong, "Clinical perspectives on reperfusion injury in acute myocardial infarction," *Am. Heart J.*, vol. 167, no. 5, pp. 637–645, May 2014.

- [2] Y. Wu, X. Yin, C. Wijaya, M.-H. Huang, and B. K. McConnell, "Acute myocardial infarction in rats," *J. Vis. Exp. JoVE*, no. 48, 2011.
- [3] F. C. McCall, K. S. Telukuntla, V. Karantalis, V. Y. Suncion, A. W. Heldman, M. Mushtaq, A. R. Williams, and J. M. Hare, "Myocardial infarction and intramyocardial injection models in swine," *Nat. Protoc.*, vol. 7, no. 8, pp. 1479–1496, Aug. 2012.
- [4] R. Klocke, W. Tian, M. T. Kuhlmann, and S. Nikol, "Surgical animal models of heart failure related to coronary heart disease," *Cardiovasc. Res.*, vol. 74, no. 1, pp. 29–38, Apr. 2007.
- [5] I. R. Efimov, V. P. Nikolski, and G. Salama, "Optical imaging of the heart," *Circ. Res.*, vol. 95, no. 1, pp. 21–33, Jul. 2004.
- [6] C. W. Zemlin, O. Bernus, A. Matiukas, C. J. Hyatt, and A. M. Pertsov, "Extracting intramural wavefront orientation from optical upstroke shapes in whole hearts," *Biophys. J.*, vol. 95, no. 2, pp. 942–50, Jul. 2008.
- [7] B. J. Caldwell, M. Wellner, B. G. Mitrea, A. M. Pertsov, and C. W. Zemlin, "Probing field-induced tissue polarization using transillumination fluorescent imaging," *Biophys. J.*, vol. 99, no. 7, pp. 2058–2066, Oct. 2010.
- [8] G. M. Faber and Y. Rudy, "Action potential and contractility changes in $[Na^+]_i$ overloaded cardiac myocytes: a simulation study," *Biophys. J.*, vol. 78, no. 5, pp. 2392–404, May 2000.
- [9] C. J. Hyatt, S. F. Mironov, F. J. Vetter, C. W. Zemlin, and A. M. Pertsov, "Optical action potential upstroke morphology reveals near-surface transmural propagation direction," *Circ. Res.*, vol. 97, no. 3, pp. 277–84, Aug. 2005.